Miniaturized Delay-Time-Enhanced Photopolymer Waveguide Hologram Module for Phased-Array Antenna

Xiaonan Chen, Zhong Shi, Lanlan Gu, Brie Howley, Yongqiang Jiang, and Ray T. Chen, *Fellow, IEEE*

***Abstract*—Miniaturized, delay-enhanced, continuous true-time delay modules based on the holographic dispersion have been designed, fabricated, and demonstrated to provide squint-free beam steering for K-, Ku-, and X-band (8–26.5 GHz) phased-array antenna systems. A novel symmetric structure is employed in the system to achieve large delays and high packaging density. The delay modules operating in the 1550-nm region provide 130 ps of continuously tunable time delay. Far-field radiation patterns measured at 18 and 22 GHz have experimentally verified the K-band beam-scanning coverage from $-45°$ to $+45°$.**

***Index Terms*—Far-field pattern, holographic grating dispersion, phased-array antenna, true-time delay, wavelength tuning.**

I. Introduction

As ONE of the key technologies in modern radar and communication systems, phased-array antennas are desirable for low visibility, high directivity, quick and accurate beam steering, and reduced power consumption. Optical true-time delay techniques have been developed to overcome the frequency squint effect, providing wide bandwidth and low electromagnetic interference compared with electronic phase-shifter approaches [1], [2]. High packaging density and the large delay coverage are considered two critical factors in a practical phased-array antenna system.

In this letter, we propose a novel symmetric structure for the true-time delay module. It has a more compact package size that is only 5% of the original structure we reported [3]. The miniaturized time delay module was experimentally confirmed to provide continuous time delays from -65 to $+65$ ps with a 1×4 subarray antenna operating at K-band (18–26.5 GHz) frequency. We describe herein the device structure of the optical true-time delay module, the measured delay-wavelength curves, and the far-field radiation patterns of the antenna system.

II. Delay Module Structure and Characteristics

The optical true-time delay modules we describe here are based upon the volume holographic grating effect. The wavelength-dependent diffraction angle out of a volume grating creates different physical paths for different input signals. The input wavelength can be precisely tuned to achieve the accurate time delay required for a continuous beam scanning. The achievable and required time delays for the antenna system are analyzed, respectively, in later discussion.

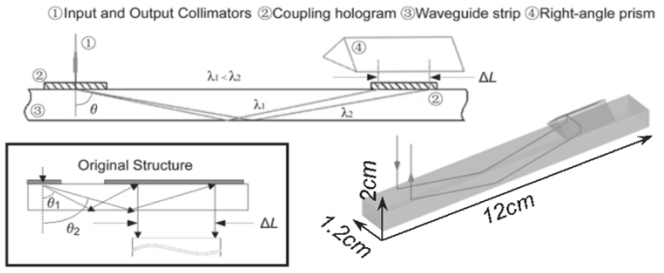

Fig. 1. Symmetric structure of the wavelength-tuning hologram waveguide-based true-time delay modules, consisting of input and output collimators with single-mode fiber pigtails, input and output dispersive holographic grating couplers, right angle prism, and glass waveguide strip. The final output position was fixed while the diffraction angle θ changed with the incident wavelength λ. The inset shows a previously proposed structure [3], in which the final output position was not fixed, which made the coupling to a single-mode fiber much more difficult.

A schematic of the true-time delay module is shown in Fig. 1. A waveguide hologram-based volume grating was used to couple an incident beam from a single-mode collimator into a glass substrate. After traveling for a one-bounce distance, the beam was surface normally coupled out by an output holographic grating. According to the coupled-wave theory [4], the diffraction angle θ is determined by the Bragg condition

$$\theta(\lambda) = 2\arcsin\left(\frac{\Lambda}{2\lambda}\right) \tag{1}$$

where Λ is the grating period of the dispersive hologram and λ is the incident wavelength. To achieve sufficient dispersive capability of the holographic grating, a large diffraction angle of 80° was chosen at the center wavelength of 1550 nm with the grating period $\Lambda = 1205.7$ nm [3]. The waveguide holograms were recorded on Dupont photopolymer film (HRF 600×001-20) by the two-beam interference method. A right angle prism was placed on top of the photopolymer to achieve required refraction angles of the recording beams which are larger than the total internal reflection angle between the air and photopolymer.

In our previous work [3] shown in one of the insets in Fig. 1, the beam was designed to be coupled out from the substrate and collected by a collimator directly. This scheme requires a sufficiently large diameter of the collimator to cover the beam po-

Manuscript received March 25, 2005; revised June 26, 2005. This work was supported by MDA, Air Force Office of Scientific Research (AFOSR), AFRL, Navy Spawar, and Defense Advanced Research Projects Agency (DARPA).

The authors are with the Microelectronics Research Center College of Engineering, The University of Texas at Austin, Austin, TX 78758 USA (e-mail: xiaonan_chen@mail.utexas.edu; zshi@micron.com; lgu@ece.utexas.edu; brie@ece.utexas.edu; yqjiang@ece.utexas.edu; rcchen@mail.utexas.edu).

Digital Object Identifier 10.1109/LPT.2005.854396

sition shift due to wavelength tuning. For a single zigzag beam path, the time delay is given by

$$t_{\text{single}}(\theta) = \frac{2nh}{(\cos\theta \cdot c)} \tag{2}$$

where n is the refractive index of the glass, h is the thickness of the substrate, and c is the light speed in free space. The maximum achievable time delay ΔT and the variation of the output position ΔL are determined by the minimum and maximum diffraction angle θ_1 and θ_2, such that

$$\Delta T = \frac{2nh}{c} \cdot \left(\frac{1}{\cos\theta_2} - \frac{1}{\cos\theta_1} \right) \tag{3}$$

$$\Delta L = 2h(\tan\theta_2 - \tan\theta_1) \tag{4}$$

where the values of θ_1 and θ_2 are limited by the amount of achievable wavelength tuning range as indicated in (1). Similarly, the time delay difference ΔT_d achieved by different delay units is derived as

$$\Delta T_d = \frac{2n\Delta h}{c} \cdot \left(\frac{1}{\cos\theta_2} - \frac{1}{\cos\theta_1} \right) \tag{5}$$

where Δh is the thickness difference between the substrates in the time delay units connected to adjacent antenna elements. Combination of equations in (3) and (5) gives

$$\Delta T = \Delta T_d \frac{h}{\Delta h}. \tag{6}$$

The time delay required to steer a phased-array antenna operating at microwave frequencies over a given range of scan angles is dependent on the element spacing d and the number of elements. Specifically, the time delay difference between adjacent antenna elements ΔT_d required to achieve beam scanning of $\pm\alpha$ degree is given by

$$\Delta T_d = 2\frac{d\sin\alpha}{c} \tag{7}$$

such that the required time delay of one delay unit is given by

$$\Delta T = 2 \cdot \left(\frac{d\sin\alpha}{c} \right) \cdot \left(\frac{h}{\Delta h} \right). \tag{8}$$

A series of delay units with equal thickness difference ($h_1 = 1$ mm, $h_2 = 3$ mm, $h_3 = 5$ mm, $h_4 = 7$ mm) were integrated as a true-time delay system, in order to use a single tunable laser to create the required delay difference ΔT_d for multiple elements in the antenna array. Calculation based on (8) gives the delay requirements (Table I) for K-, Ku-, and X-band phased-array antenna systems. For the original delay module described in [3], the achievable wavelength tuning range and the device parameters were designed as $\lambda_2 - \lambda_1 = 12$ nm, $\theta_1 = 77.5°$, $\theta_2 = 82°$, $\Delta T = 128$ ps, $\Delta L = 36.5$ mm, which allowed $-37°$–$+37°$ beam scanning coverage for the X-band phased-array antenna system. It is seen from the calculation that a collimator with an effective diameter larger than 36.5 mm has to be used in the system to cover the large ΔL value. Collimators with such a large numerical aperture introduce a few problems such as large size multimode outputs and low coupling efficiency, which make it impractical for real applications.

In the new delay module described here, the output beam is first coupled into a right-angle prism, which reflected the light beam and formed an additional reversed beam path within the substrate. Having bidirectional symmetric beam paths causes the final output position to be fixed. Miniaturized collimators with single-mode fiber pigtails could then be used to collect the output signal. This symmetric structure provides a much more compact packaging size (12 × 2 × 1.2 cm) and less coupling loss (2 dB) compared with the original single-path design (15 × 15 × 3 cm, 10 dB), where multimode-to-single-mode conversion is required. Furthermore, in the novel symmetric structure, the time delay is doubled due to the backward bounce of the light beam. With the same requirement of maximum achievable time delay, the incident wavelength tuning range is reduced compared with the original single-path structure.

TABLE I
TIME DELAY REQUIREMENT FOR MICROWAVE PHASED ARRAY ANTENNAS
($\Delta h = 2$ mm, $h_3 = 5$ mm)

Operating Band	Antenna Element Spacing (d)	Beam Scanning Angle (α)	Time Delay Requirement (ΔT)
K-band (18-26.5 GHz)	7 mm	± 45°	82ps
Ku-band (12.5-18 GHz)	10 mm	± 45°	118ps
X-band (8-12.5 GHz)	13 mm	± 37°	130ps

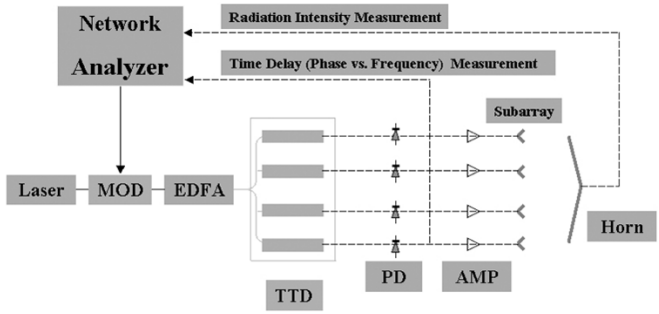

Fig. 2. Block diagram for time delay (phase versus frequency) measurement and system demonstration. Tunable laser: used to provide light with wavelength tunable from 1544 to 1556 nm. Network analyzer: used to measure the phase and intensity of the RF signal. PD: four 40-GHz photodetectors. AMP: four two-stage RF amplifiers. MOD: 40-GHz polymer Mach–Zehnder intensity modulator. TTD: True-time-delay modules of the type depicted in Fig. 1.

III. MEASUREMENT AND RESULTS

The measurement system used to evaluate the new delay modules is presented in Fig. 2. An HP network analyzer (8510C) was used to measure radio-frequency (RF) phase as a function of RF frequency, from which we could calculate the experimental time delay. A C-band (1530–1560 nm) tunable laser was modulated by an external 40-GHz polymer Mach–Zehnder intensity modulator, which was driven by Port 1 of the network analyzer. The modulated signal was fed into the delay device and then converted to an electrical signal by the 40-GHz PIN photodetectors. After amplification, the signal was received by Port 2 of the network analyzer. The RF phase versus RF frequency as a function of incident optical wavelength is shown in Fig. 3(a). Linearity of the measured phase versus frequency characteristic confirms that the measured time delays are independent of RF frequencies. The corresponding time delays are shown in Fig. 3(b). Compared with the original structure, the new structure provides doubled maximum achievable time

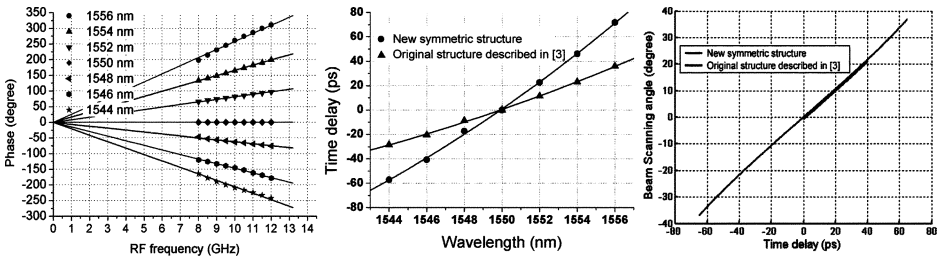

(a) (b) (c)

Fig. 3. (a) Measured (points) and simulated (lines) results of RF phase versus RF frequency. (b) Measured (points) and simulated (lines) results of time delay versus incident wavelength compared with original structure. (c) Comparison of simulated beam scanning angle versus controlled time delay for X-band elements.

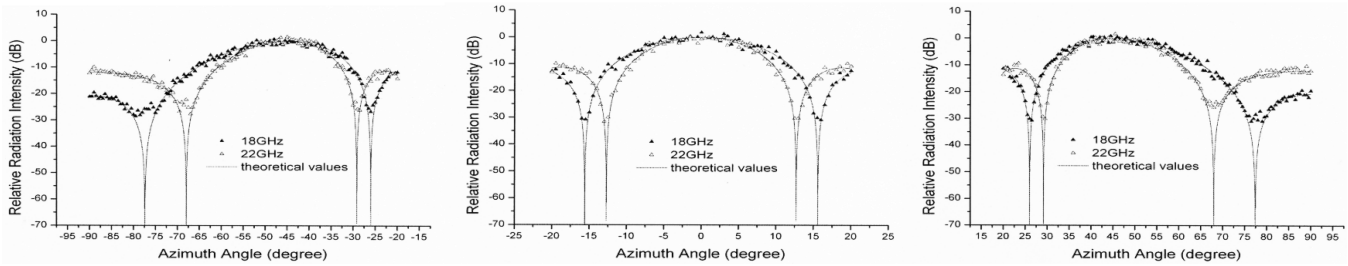

Fig. 4. Measured and simulated radiation patterns at 18 and 22 GHz with beam steering angle $\alpha = (-45°, 0°, +45°)$. The broadside radiation axis of the antenna array was precisely rotated and situated at the azimuth angle, relative to the horn's broadside radiation axis.

delay within the same incident wavelength range that is consistent with the simulation results. The simulated beam scanning angle versus time delay curve for an X-band antenna is shown in Fig. 3(c). With the enhanced delay coverage, the demonstrated four-element phased-array antenna system can cover a larger beam scanning angle, $-37° \rightarrow +37°$ for X-band antenna elements $(d = 13$ mm$)$ and $-45° \rightarrow +45°$ for K-band antenna elements $(d = 7$ mm$)$. At the receiving end of the system measurement setup, an antenna horn was used to receive the phased-array radiation signal. The broadside radiation axis of the antenna array was precisely rotated and situated at the azimuth angle (Fig. 4), relative to the horn's broadside radiation axis. The measured radiation patterns and corresponding simulation results for $\alpha = (-45°, 0°, +45°)$ at K-band are shown in Fig. 4. At 18 and 22 GHz, the peaks coincide confirming the beam-squint-free character of the true-time delay modules.

IV. Applications in Large Array System

The optical modules proposed in this letter can be cascade-connected to achieve long enough time delay for real-world PAA systems that usually have thousands of elements. The schematic is presented in Fig. 5. Each delay unit is composed of one delay module and one beam splitter. All delay units are cascade-connected and the output of each splitter is fed into the following delay unit, such that each delay module provides the required delay difference ΔT_d for adjacent antenna elements. The splitting ratio of each splitter is designed to achieve equalized output optical power for each antenna element. The wavelength accuracy of the tunable laser (0.001 nm) and the dispersion of delay modules (12.5 ps/nm) determine the delay resolution (0.0125 ps) and beam scanning accuracy (0.022°) of the cascaded system.

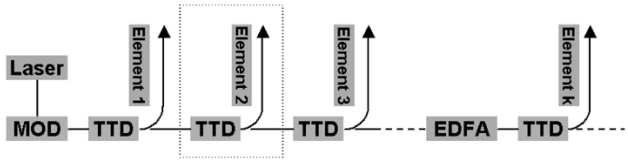

Fig. 5. Cascaded architecture of delay units for large array antennas. Each delay module provides the required delay difference ΔT_d for adjacent antenna elements.

V. Conclusion

A miniaturized, continuously tunable, optical true-time delay module has been fabricated, packaged, evaluated, and integrated with a subarray antenna system. A novel symmetric structure was introduced to keep the output beam position fixed and provide doubled maximum achievable time delay. We also proposed a cascaded time delay architecture for the applications of our true-time delay module in large phased-array antenna systems.

References

[1] D. Dolfi, J. P. Huignard, and M. Baril, "Optically controlled true time delays for phased array antenna," *Proc. SPIE*, vol. 1102, pp. 152–161, 1989.

[2] W. Ng, A. A. Walston, G. L. Tangonan, J. J. Lee, I. L. Newberg, and N. Bernstein, "The first demonstration of an optically steered microwave phased array antenna using true time-delay," *J. Lightw. Technol.*, vol. 9, no. 9, pp. 1124–1131, Sep. 1991.

[3] Z. Shi, L. Gu, B. Howley, Y. Jiang, Q. Zhou, R. T. Chen, Y. Chen, H. R. Fetterman, C. Lee, and G. Brost, "True-time-delay modules based on single tunable laser in conjunction with waveguide hologram for phased array antenna application," *Opt. Eng.*, vol. 44, p. 084301, Aug. 2005.

[4] H. Kogelnik, "Coupled wave theory for thick hologram gratings," *Bell Syst. Tech. J.*, vol. 48, pp. 2909–2947, 1969.